Distributed control for position and attitude tracking of quadrotor formations Using Lyapunov transformations

Miguel Araújo[1*] and Paulo Oliveira[1]

[1]Department of Electrotechnical and Computer Engineering, Instituto Superior Técnico, Av. Rovisco Pais, Nº 1, Lisbon, 1049-001, Portugal.

*Corresponding author(s). E-mail(s): ist199533@tecnico.ulisboa.pt;
Contributing authors: paulo.j.oliveira@tecnico.ulisboa.pt;

Abstract

In this paper, a non-linear feedback control strategy for quadrotor trajectory tracking is employed to design a distributed controller for a group of identical vehicles, in order to achieve formation trajectory tracking. The formation controller uses notions of graph algebra and consensus theory. Sufficient conditions for group stability are given regarding the individual stability of the vehicles and information flow. The controller design benefits from Lyapunov transformations to render the non-linear dynamics into LTI systems without any approximations, in which is possible to use well known linear tools of analysis and design such as LQR. The overall controller is proven to be stable, to ensure 3D trajectory tracking of constant velocity trajectories without static error and to reject unknown constant disturbances from wind.

Keywords: Nonlinear control, Consensus, Distributed Control, Quadrotor

1 Introduction

With the continuous development of the technology of autonomous vehicles, multi-vehicle applications are increasingly more desirable and relevant in various industries. It comes to no surprise that the study of robust control methods for these kinds of problems spark a peculiar interest, since the dynamically decoupled vehicles, with limited knowledge about the whole group, must act coordinated.

Classical solutions usually followed the "leader-follower" approach or the "virtual leader" approach due to their simplicity. However, problems in group performance and in computational load lead to the research of broader forms of communicability between vehicles and more general means of distributed control. In particular, in [1], [2] and [3], ideas from graph theory were used in control theory to develop criterion of stability in consensus problems, both in linear and non-linear settings, resulting in a solid theory that also includes the classical solutions, but opened path to many more possibilities.

Bigger cooperation between vehicles alleviates the individual computational burden while enhancing robustness against external factors that may affect the information flow within the group, paving the way for more complex applications with an increasing number of vehicles. For instance, distributed control for the rendezvous of vehicles was explored in [4] and [5].

Naturally, the design of group control solutions mustn't be dissociated of a careful control analysis of each individual vehicle. This paper will explore the control tools developed in [6] for a single quadrotor vehicle. There, the employment of non-linear Lyapunov transformations, as studied in [7], allowed the design of a robust non-linear control law using common linear methods without approximations. In this work, the focus is to extend this control law to distributed control of multi-vehicle groups and study it's tracking performance and robustness facing disturbances.

This paper is organized as follows: section 2 introduces the vehicle kinematic and dynamic equations, as well as the problem statement and objective. Section 3 presents the necessary notions and results on consensus theory to develop the distributed controller. Section 4 provides the design of the position tracking controller for the whole formation that allows the tracking of a constant velocity trajectory without static errors and rejection of constant disturbances. In this section, an individual attitude controller framework is also presented. In section 5, a simulation is presented in order to experimentally confirm the theoretical findings. Concluding remarks will be presented in Section 6.

Notation

In this paper, vectors will be denoted by bold lower-case letters (e.g. $\boldsymbol{u}$, $\boldsymbol{x}$), matrices will be represented by bold upper-case letters (e.g. $\boldsymbol{R}, \boldsymbol{L}$) and the i-th element of a vector is denoted $\boldsymbol{x}_i$. The symbol $\mathbf{0}$ symbolizes a matrix full of zeros, with appropriate dimensions, and $\boldsymbol{I}_n$ represents an $n \times n$ identity matrix. Furthermore, the unit vectors aligned with the x, y and z axis are, respectively, $\boldsymbol{e}_1$, $\boldsymbol{e}_2$ and $\boldsymbol{e}_3$. The time derivative of a quantity s is denoted by $\dot{s}$ and $\|\boldsymbol{x}\|, \boldsymbol{x} \in \mathbb{R}^n$, denotes the Euclidian norm of vectors. In $\mathbb{R}^3$, $[\boldsymbol{v}\times]$ defines the skew-symmetric of a generic vector $\boldsymbol{v}$ as

$$[\boldsymbol{v}\times] = \begin{bmatrix} 0 & -\boldsymbol{v}_3 & \boldsymbol{v}_2 \\ \boldsymbol{v}_3 & 0 & -\boldsymbol{v}_1 \\ -\boldsymbol{v}_2 & \boldsymbol{v}_1 & 0 \end{bmatrix}.$$

$\{E\}$ represents a generic coordinate frame and, in particular, $\{I\}$ denotes the inertial frame of reference and $\{B\}$ denotes the vehicle's body frame. Finally, the $\otimes$ symbol will be used to denote the Kronecker product between matrices and, for a succession of k square matrices $\boldsymbol{A}_i \in \mathbb{R}^{n\times n}$, $\hat{\boldsymbol{A}} \in \mathbb{R}^{kn\times kn}$ will be defined as

$$\hat{\boldsymbol{A}} = \begin{bmatrix} \boldsymbol{A}_1 & \dots & \mathbf{0} \\ \vdots & \ddots & \vdots \\ \mathbf{0} & \dots & \boldsymbol{A}_k \end{bmatrix}.$$

2 Problem Formulation

2.1 Quadrotor Dynamics and Kinematics

Consider the quadrotor vehicle model represented in Fig. 1. It is equipped with four identical motors and propellers symmetrically distributed along the body, which are able to generate a thrust force and a torque normal to the rotor plane. Let the vehicle's body frame be located at its centre of mass. The differential equations that describe the kinematics and dynamics of this vehicle, with possible wind perturbations, are defined as

$$\dot{\boldsymbol{p}} = \boldsymbol{R}\boldsymbol{v}, \tag{1}$$

$$\dot{\boldsymbol{v}} = -[\boldsymbol{\omega}\times]\boldsymbol{v} - \frac{T}{m}\boldsymbol{e}_3 + \boldsymbol{R}^T g\boldsymbol{e}_3 + \boldsymbol{R}^T\boldsymbol{d}, \tag{2}$$

$$\dot{\boldsymbol{q}} = \frac{1}{2}\boldsymbol{\Omega}(\boldsymbol{\omega})\boldsymbol{q}, \tag{3}$$

$$\dot{\boldsymbol{\omega}} = -\boldsymbol{J}^{-1}[\boldsymbol{\omega}\times]\boldsymbol{J}\boldsymbol{\omega} + \boldsymbol{J}^{-1}\boldsymbol{\tau}, \tag{4}$$

being $m \in \mathbb{R}$ the total mass of the system, $\boldsymbol{J} \in \mathbb{R}^{3\times3}$ the inertia matrix with respect to $\{B\}$, $\boldsymbol{R} \in \mathrm{SO}(3)$ the rotation matrix from $\{B\}$ to $\{I\}$ following the Tait-Bryan sequence Z-Y-X, $\boldsymbol{p} \in \mathbb{R}^3$ the position of the centre of mass in $\{I\}$, $\boldsymbol{v} \in \mathbb{R}^3$ the velocity of the centre of mass relative to $\{I\}$, expressed in $\{B\}$, $\boldsymbol{q} \in \mathbb{R}^4$ the attitude in quaternion form, where $\boldsymbol{q} = \begin{bmatrix}\boldsymbol{q}_v^T & q_4\end{bmatrix}^T$, $\boldsymbol{\omega} \in \mathbb{R}^3$ the angular velocity relative to $\{I\}$, expressed in $\{B\}$, $\boldsymbol{d} \in \mathbb{R}^3$ the perturbations caused by wind in $\{I\}$, $T \in \mathbb{R}_{\geq 0}$ the total generated thrust, $\boldsymbol{\tau} \in \mathbb{R}^3$ the total generated torque, and $\boldsymbol{\Omega}(\boldsymbol{\omega}) = \begin{bmatrix} -[\boldsymbol{\omega}\times] & \boldsymbol{\omega} \\ -\boldsymbol{\omega}^T & 0 \end{bmatrix}$.

2.2 Problem formulation

Consider a set of n identical quadrotor vehicles, each with individual dynamics described in Eqs. (1) to (4). Suppose that each vehicle is able to measure the relative position of a subset of other vehicles, effectively establishing an information graph $G = (\mathcal{V}, \mathcal{E}, \boldsymbol{\mathcal{A}})$. Here, $\mathcal{V}$ is the set of vertices v_i in the graph (the set of vehicles) and $\mathcal{E}$ is

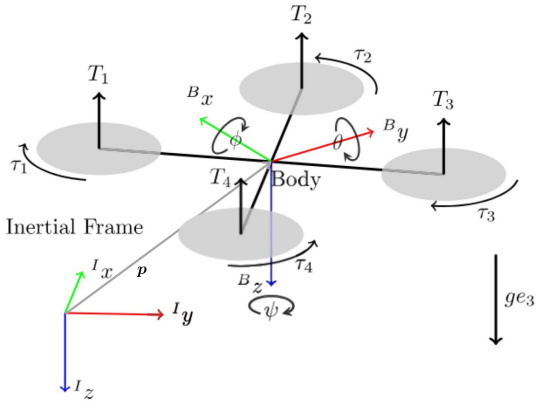

Fig. 1: Diagram of the quadrotor

the set of edges (v_i, v_j) (connection from vehicle i to vehicle j). Lastly, let $a_{ij} \in \mathbb{R}_{\geq 0}$ denote the weight of the edge (v_i, v_j) and define $\boldsymbol{\mathcal{A}} = [a_{ij}]$ as the adjacency matrix of the graph. The following assumption will allow for easier calculations without loss of generality.

Assumption 1 *The information graph does not contain any self-loops, that is,* $a_{ii} = 0,\ i \in \{1, \ldots, n\}$.

Design a controller for each vehicle that allows formation control and trajectory tracking of a prescribed trajectory $\boldsymbol{p}_d \in C^4$, followed by a specified heading angle $\psi_d \in C^2$, that is able to reject constant wind perturbations. Additionally, assume that each vehicle i has a sensor set that is able to exactly measure, in real-time, the relative position of vehicle j, $(\boldsymbol{p}_j - \boldsymbol{p}_i)$, its velocity $\boldsymbol{v}_i$, its attitude $\boldsymbol{q}_i$ and its angular velocity $\boldsymbol{\omega}_i$. Nowadays, in commercially available quadcopters these quatities can be obtained resorting to motion sensors installed onboard, namelly GPS, rate gyros, magnetometers and accelerometers ([8]). In order to guarantee a well-posed control law, the following assumption will be established.

Assumption 2 *The angular velocities* $\boldsymbol{\omega}_i$ *and angular accelerations* $\dot{\boldsymbol{\omega}}_i$*, with* $i \in \{1, ..., n\}$*, are bounded signals.*

3 Consensus Theory

Consider an algebraic directed graph $G_x = (\mathcal{V}, \mathcal{E}, \boldsymbol{\mathcal{A}}, \boldsymbol{x})$ consisting of n nodes, with $\boldsymbol{x}_i \in \mathbb{R},\ i \in \{1, ..., n\}$ denoting the value of node v_i. It is said that the nodes reach a consensus when $\boldsymbol{x}_i = \boldsymbol{x}_j$, for all $i \neq j$.

Define the out-degree of node v_i as

$$\deg_{out}(v_i) = \sum_{j=1}^{n} a_{ij}. \tag{5}$$

The *degree matrix* $\boldsymbol{\Delta} = [\Delta_{ij}]$ is constructed by concatenating the values of the out-degrees of each node in the main diagonal, with $\Delta_{ii} = \deg_{out}(v_i)$ and $\Delta_{ij} = 0,\ \forall i \neq j$. It is possible to define the *Laplacian matrix* associated with G_x as

$$\boldsymbol{L} = \boldsymbol{\Delta} - \boldsymbol{\mathcal{A}}. \tag{6}$$

Remark 1 By construction, all the elements of each row of $\boldsymbol{L}$ sum to zero. Therefore, $\boldsymbol{L}$ has a zero eigenvalue corresponding to the eigenvector $\boldsymbol{w} = \begin{bmatrix} 1 & \ldots & 1 \end{bmatrix}^T$. In other words, the rank of $\boldsymbol{L}$ is lower than n.

A graph is said to be *strongly connected* if and only if every pair of nodes in the graph can be connected via a path that respects the orientation of the edges. In [2], a very important conclusion is proven in the case of strongly connected graphs.

Theorem 1 *Let* $G = (\mathcal{V}, \mathcal{E}, \boldsymbol{\mathcal{A}})$ *be a weighted directed graph with Laplacian* $\boldsymbol{L}$*. Then* $\text{rank}(\boldsymbol{L}) = n - 1$ *if and only if* G *is strongly connected.*

Another important theorem proven in [2], based on the Geršgorin disk theorem, is also presented.

Theorem 2 *Let* $G = (\mathcal{V}, \mathcal{E}, \boldsymbol{\mathcal{A}})$ *be a weighted directed graph with Laplacian* $\boldsymbol{L}$*. Let* $d_{max}(G) = \max_i \deg_{out}(v_i)$*, with* $i \in \{1, ..., n\}$*. Then all the eigenvalues of* $\boldsymbol{L}$ *are located in the following disk*

$$D(G) = \{z \in \mathbb{C} : |z - d_{max}(G)| \leq d_{max}(G)\} \tag{7}$$

With the conclusions expressed in these two theorems, we may then draw the following result.

Theorem 3 *Consider a strongly connected algebraic graph $G_x = (\mathcal{V}, \mathcal{E}, \boldsymbol{\mathcal{A}}, \boldsymbol{x})$ with n nodes and a corresponding Laplacian matrix $\boldsymbol{L}$. Let each value $\boldsymbol{x}_i$, with $i \in \{1, ..., n\}$, be defined by the dynamics:*

$$\begin{cases} \dot{\boldsymbol{x}}_i \equiv \dot{\boldsymbol{x}}_{i_1} = \boldsymbol{x}_{i_2} \\ \dot{\boldsymbol{x}}_{i_2} = \boldsymbol{x}_{i_3} \\ \vdots \\ \dot{\boldsymbol{x}}_{i_m} = \boldsymbol{u}_i \end{cases}, \tag{8}$$

where $\boldsymbol{u}_i$ is the input of node i. The control law

$$\boldsymbol{u} = -\boldsymbol{L}\boldsymbol{x}, \tag{9}$$

is stable for $m = 1$ and all nodes will reach a consensus around some value α. For $m = 2$ the system is marginally stable if $\boldsymbol{L}$ has real eigenvalues. All other cases lead to an unstable scenario.

Proof With this control law, the full dynamics of the whole graph, described by the vector $\boldsymbol{x}_f = (\boldsymbol{x}_{1_1}, ..., \boldsymbol{x}_{n_1}, ..., \boldsymbol{x}_{1_m}, ..., \boldsymbol{x}_{n_m})$, can be written in the following space-state form:

$$\dot{\boldsymbol{x}}_f = \begin{bmatrix} \boldsymbol{0} & \boldsymbol{I}_n & \boldsymbol{0} & \dots & \boldsymbol{0} \\ \boldsymbol{0} & \boldsymbol{0} & \boldsymbol{I}_n & \dots & \boldsymbol{0} \\ \vdots & \vdots & \vdots & \ddots & \vdots \\ \boldsymbol{0} & \boldsymbol{0} & \boldsymbol{0} & \dots & \boldsymbol{I}_n \\ -\boldsymbol{L} & \boldsymbol{0} & \boldsymbol{0} & \dots & \boldsymbol{0} \end{bmatrix} \boldsymbol{x}_f \equiv \boldsymbol{M}\boldsymbol{x}_f. \tag{10}$$

To evaluate the eigenvalues of $\boldsymbol{M}$, the Schur's formula must be used, which states that, by writing $\boldsymbol{M} - \lambda \boldsymbol{I}_{kn}$, with $\lambda \in \mathbb{C}$, as a block matrix $\begin{bmatrix} \boldsymbol{P} & \boldsymbol{Q} \\ \boldsymbol{R} & \boldsymbol{S} \end{bmatrix}$, with $\boldsymbol{S}$ invertible, the determinant can be computed as

$$\det(\boldsymbol{M} - \lambda \boldsymbol{I}_{mn}) = \det(\boldsymbol{S}) \det(\boldsymbol{P} - \boldsymbol{Q}\boldsymbol{S}^{-1}\boldsymbol{R}). \tag{11}$$

Choosing

$$\begin{cases} \boldsymbol{P} = \begin{bmatrix} -\lambda \boldsymbol{I}_n & \boldsymbol{I}_n & \dots & \boldsymbol{0} & \boldsymbol{0} \\ \vdots & \vdots & \ddots & \vdots & \vdots \\ \boldsymbol{0} & \boldsymbol{0} & \dots & -\lambda \boldsymbol{I}_n & \boldsymbol{I}_n \\ \boldsymbol{0} & \boldsymbol{0} & \dots & \boldsymbol{0} & -\lambda \boldsymbol{I}_n \end{bmatrix} \\ \boldsymbol{Q} = \begin{bmatrix} \boldsymbol{0} & \dots & \boldsymbol{I}_n \end{bmatrix}^T \\ \boldsymbol{R} = \begin{bmatrix} -\boldsymbol{L} & \dots & \boldsymbol{0} \end{bmatrix} \\ \boldsymbol{S} = -\lambda \boldsymbol{I}_n \end{cases}, \tag{12}$$

and continuously applying Schur's formula, the determinant is found to be

$$\det(\boldsymbol{M} - \lambda \boldsymbol{I}_{mn}) = \det(-\boldsymbol{L} - \lambda^m \boldsymbol{I}_n). \tag{13}$$

Let λ_L denote the eigenvalues of $\boldsymbol{L}$. Making the above determinant equal to 0, it is possible to obtain the eigenvalues of $\boldsymbol{M}$ with

$$\lambda = \sqrt[m]{\lambda_L} e^{\frac{\pi + 2k\pi}{m} i}, \ k \in \mathbb{Z}. \tag{14}$$

With theorem 2, it is known that all values of λ_L must lay in the right complex half-plane, which directly leads to the conclusion that the control law is stable for $m = 1$. In addition, from theorem 1, $\boldsymbol{L}$ only has one eigenvalue in 0 corresponding to the eigenvector $\boldsymbol{w} = \begin{bmatrix} 1 & ... & 1 \end{bmatrix}^T$, which is the case where all the nodes have the same value. Thus, the conclusion is that all the disagreements between nodes are associated with the non-zero eigenvalues of $\boldsymbol{M}$ which are proven to lay on the left half-plane complex. As such, the disagreements converge exponentially to 0, which means that the nodes reach a consensus around some value α.

For $m = 2$, it can be seen that, for real eigenvalues λ_L, the eigenvalues of $\boldsymbol{M}$ will lay on the imaginary axis, rendering the system marginally stable. All other cases will cause $\boldsymbol{M}$ to have eigenvalues on the right complex half-plane, making this control law unstable. □

As it will be seen, the vehicles studied in this paper are similar to nodes with dynamics described by a pure integrator since, in order to control the position, it is necessary to act on the velocity. According to 3, the control law $\boldsymbol{u} = -\boldsymbol{L}\boldsymbol{x}$ would allow a marginally stable outer loop between any number of vehicles with those kinds of dynamics where information flows through a strongly connected graph. However, in tracking problems, it is very usual to add integrative states to position in order to drive static errors to zero. This would add an unstable 3rd order contribution to the already marginally stable 2nd component, which would make the outer loop unstable.

Do note that the vehicles are not pure integrators and have their own internal dynamics which, if stable, might compensate the instability caused by the outer loop. This raises the question of how stable must each node be in order to mitigate the instabilities caused the group controller. In order to give an answer to this question, it is useful to start with Bendixon's theorem ([9]).

Theorem 4 (Bendixon) *Let $\boldsymbol{A}$ be a real valued $n \times n$ matrix, with complex eigenvalues λ_i, $i \in \{1, ..., n\}$. Define $\boldsymbol{Q} = \frac{1}{2}(\boldsymbol{A} + \boldsymbol{A}^T)$ and denote λ_+ and λ_- as, respectively, the greatest and lowest eigenvalues of $\boldsymbol{Q}$. Then*

$$\lambda_- \leq \mathcal{R}e\{\lambda_i\} \leq \lambda_+. \tag{15}$$

Following the above conclusions, a sufficient condition may be drawn for the stability of the

sum of two systems, with at least one of them being individually stable.

Theorem 5 *Consider a stable dynamic system, $\dot{\boldsymbol{x}} = \boldsymbol{f}(\boldsymbol{x})$, that admits a Lyapunov function V_f that satisfies*

1. $V_f(\boldsymbol{x}) \geq \epsilon \boldsymbol{x}^T \boldsymbol{x},\ \forall_{\boldsymbol{x}\in\mathbb{R}^n}$;
2. $\dot{V}_f(\boldsymbol{x}) \leq -\lambda V_f(\boldsymbol{x}),\ \forall_{\boldsymbol{x}\in\mathbb{R}^n}$.

Consider as well the linear system $\dot{\boldsymbol{x}} = \boldsymbol{A}\boldsymbol{x}$ and let λ_+ denote the majorant of the real part of the eigenvalues of $\boldsymbol{A}$. The sum of these systems,

$$\dot{\boldsymbol{x}} = \boldsymbol{f}(\boldsymbol{x}) + \boldsymbol{A}\boldsymbol{x}, \tag{16}$$

is stable if $\lambda_+ < \lambda\epsilon$.

Proof Regarding system 16, let $V(\boldsymbol{x}) = V_f(\boldsymbol{x}) + \frac{1}{2}\boldsymbol{x}^T\boldsymbol{x}$ be a candidate Lyapunov function. It is clear that

1. $V(\boldsymbol{0}) = 0$;
2. $V(\boldsymbol{x}) > \boldsymbol{x},\ \forall_{\boldsymbol{x}\neq\boldsymbol{0}}$;
3. $\dot{V}(\boldsymbol{x}) \leq -\lambda V_f(\boldsymbol{x}) + \boldsymbol{x}^T\boldsymbol{A}\boldsymbol{x},\ \forall_{\boldsymbol{x}\neq\boldsymbol{0}}$.

From theorem 4, with λ_+ as the largest real component of the eigenvalues of $\boldsymbol{A}$,

$$\dot{V}(\boldsymbol{x}) \leq -\lambda V_f(\boldsymbol{x}) + \lambda_+ \boldsymbol{x}^T\boldsymbol{x}. \tag{17}$$

If $\boldsymbol{A}$ only has eigenvalues on the left complex halfplane, then, directly, V is a Lyapunov function and the system is stable. However, if $\boldsymbol{A}$ has eigenvalues with positive real part, then, noting that $V_f \geq \epsilon\boldsymbol{x}^T\boldsymbol{x}$,

$$\dot{V}(\boldsymbol{x}) \leq (\lambda_+ - \lambda\epsilon)\boldsymbol{x}^T\boldsymbol{x} \tag{18}$$

Thus, if $\lambda_+ < \lambda\epsilon$, V is a valid Lyapunov function and system 16 is stable □

With this last result, it is now known a sufficient condition for stability of a global controller comprised as the sum of a stable inner loop and an unstable outer loop. Do note that, if both loops are stable, then the global system is directly stable as well. Moreover, a special case is obtained when both systems are linear.

Corollary 1 *Consider a stable system $\dot{\boldsymbol{x}} = \boldsymbol{A}\boldsymbol{x}$ and an unstable system $\dot{\boldsymbol{x}} = \boldsymbol{B}\boldsymbol{x}$. Let λ_{A_+} be the majorant of the real part of the eigenvalues of A and λ_{B_+} the majorant of the real part of the eigenvalues of B. The system*

$$\dot{\boldsymbol{x}} = (\boldsymbol{A} + \boldsymbol{B})\boldsymbol{x} \tag{19}$$

is stable if $\lambda_{B_+} < |\lambda_{A_+}|$

The conclusion drawn from this section is that it is possible to simply add an external control loop for formation control to the internal dynamics of each node, as long as the former is not too unstable, meaning that the controller design can start with the internal control loop and then pass to the external one. Do note that the nodes needn't have the same internal dynamics.

As a last remark, note that the overall performance for the group agreement task is related with the eigenvalue of $\boldsymbol{L}$ with the smallest real part (different from 0). This eigenvalue can be shown to be larger for denser networks and smaller for sparser ones ([2]).

4 Controller Design

With the conclusions drawn from the previous section, to tackle the problem stated in 2.2, a nonlinear internal control law will be derived in order to make each vehicle internally stable around an equilibrium position. Furthermore, an external control law will be proposed in order to make the position of each vehicle in the formation controllable, making use of the communications they are able to have between themselves. Through a set of Lyapunov nonlinear transformations ([7]), the dynamics becomes linear, allowing the use of well-known linear techniques.

4.1 Position Tracking Control

Suppose the vehicles communicate between each other following a strongly connected algebraic graph $G_p = (\mathcal{V}, \mathcal{E}, \boldsymbol{\mathcal{A}}, \boldsymbol{p})$, where $\boldsymbol{p}$ is the position vectors of all vehicles in the formation. Assume that the graph is such that its corresponding Laplacian matrix, $\boldsymbol{L}$ has only real eigenvalues. To ensure tracking, imagine the presence of a "virtual" vehicle, which follows the desired trajectory perfectly and is able to inform a subset of vehicles about its position in real-time. This creates a new information graph based on the last one, $G' = (\mathcal{V}', \mathcal{E}', \boldsymbol{\mathcal{A}}', \boldsymbol{p})$., with

$$\boldsymbol{\mathcal{A}}' = \begin{bmatrix} 0 & a_{12} & \dots & a_{1n} & b_1 \\ a_{21} & 0 & \dots & a_{2n} & b_2 \\ \vdots & \vdots & \ddots & \vdots & \vdots \\ a_{n1} & a_{n2} & \dots & 0 & b_n \\ 0 & 0 & \dots & 0 & 0 \end{bmatrix}, \tag{20}$$

where the values v_i are the weights of the edges that connect the virtual vehicle to the vehicles in the formation. The error vector for the i-th vehicle may be defined as

$$\boldsymbol{z}_i = \sum_{j=1}^{n}(a_{ij}(\boldsymbol{p}_i - \boldsymbol{p}_j - \boldsymbol{h}_{ij}) + b_i(\boldsymbol{p}_i - \boldsymbol{p}_d - \boldsymbol{h}_{id})) \quad (21)$$

where, $\boldsymbol{p}_d$ is the desired trajectory. Vectors $\boldsymbol{h}_{ij}$ represent an offset that should exist between the i-th and the j-th vehicle, and vector $\boldsymbol{h}_{id}$ is the offset that should exist between the i-th vehicle and the virtual vehicle. These vectors may be interpreted as the relative position the vehicles should have amongst themselves in steady-state, thus prescribing the shape of the formation along time. Concatenating these vectors into a single one, $\boldsymbol{z} = \begin{bmatrix}\boldsymbol{z}_1 & ... & \boldsymbol{z}_n\end{bmatrix}^T$, leads to

$$\boldsymbol{z} = (\boldsymbol{L}' \otimes \boldsymbol{I}_3)\boldsymbol{p} - \boldsymbol{h} - (\boldsymbol{b} \otimes \boldsymbol{I}_3)\boldsymbol{p}_d \equiv \boldsymbol{L}'_3\boldsymbol{p} - \boldsymbol{z}_{ref}. \quad (22)$$

In this equation, $\boldsymbol{L}'$ represents the Laplacian matrix of the graph G'_p without the row and column referring to the virtual vehicle. This matrix can be constructed using the Laplacian matrix of G_p, $\boldsymbol{L}$, by doing

$$\boldsymbol{L}' = \boldsymbol{L} + \begin{bmatrix} b_1 & ... & 0 \\ \vdots & \ddots & \vdots \\ 0 & ... & b_n \end{bmatrix}. \quad (23)$$

Furthermore, the presence of the Kronecker product comes from the fact that the position has three components. In practice, there exists three identical graphs but with different algebraic quantities, one for each position coordinate in tridimensional trajectories. Finally, the vector $\boldsymbol{h}$ concatenates all the offsets for a particular vehicle, with

$$\boldsymbol{h}_i = \sum_{j=1}^{n}(a_{ij}\boldsymbol{h}_{ij} + b_i\boldsymbol{h}_{id}). \quad (24)$$

Remark 2 The null eigenvalue that was present on $\boldsymbol{L}$ by construction disappears once $\boldsymbol{L}'$ is formed. That null eigenvalue represented the fact that the consensus to where the vehicles would arrive was uncontrollable due to the absence of absolute measurements of the position. Once those measurements exist, it is possible to set what should be the value of the consensus.

Remark 3 Due to construction, matrix $\boldsymbol{L}'_3$ will have the same eigenvalues as $\boldsymbol{L}'$, each with an algebraic multiplicity of 3.

Define an integrative state $\boldsymbol{\eta}$ such that $\dot{\boldsymbol{\eta}} = \boldsymbol{z}$. Attending to equations (1) and (2) and with $\boldsymbol{u}_i = -\frac{T_i}{m}\boldsymbol{e}_3 + \boldsymbol{R}_i^T g\boldsymbol{e}_3$, the full dynamics of the drone formation can be written as

$$\begin{bmatrix}\dot{\boldsymbol{v}}\\ \dot{\boldsymbol{z}}\\ \dot{\boldsymbol{\eta}}\end{bmatrix} = \begin{bmatrix}\widehat{[\boldsymbol{\omega}\times]} & \boldsymbol{0} & \boldsymbol{0}\\ \boldsymbol{L}'_3\hat{\boldsymbol{R}} & \boldsymbol{0} & \boldsymbol{0}\\ \boldsymbol{0} & \boldsymbol{I}_{3n} & \boldsymbol{0}\end{bmatrix}\begin{bmatrix}\boldsymbol{v}\\ \boldsymbol{z}\\ \boldsymbol{\eta}\end{bmatrix} + \begin{bmatrix}\boldsymbol{I}_{3n}\\ \boldsymbol{0}\\ \boldsymbol{0}\end{bmatrix}\boldsymbol{u} + \begin{bmatrix}\boldsymbol{R}^T\\ \boldsymbol{0}\\ \boldsymbol{0}\end{bmatrix}\boldsymbol{d} + \begin{bmatrix}\boldsymbol{0}\\ \boldsymbol{I}_{3n}\\ \boldsymbol{0}\end{bmatrix}\dot{\boldsymbol{z}}_{ref}. \quad (25)$$

Consider the following Lyapunov transformation ([6])

$$\begin{bmatrix}\boldsymbol{x}_v\\ \boldsymbol{x}_z\\ \boldsymbol{x}_\eta\end{bmatrix} = \begin{bmatrix}\hat{\boldsymbol{R}} & \boldsymbol{0} & \boldsymbol{0}\\ \boldsymbol{0} & \boldsymbol{I}_{3n} & \boldsymbol{0}\\ \boldsymbol{0} & \boldsymbol{0} & \boldsymbol{I}_{3n}\end{bmatrix}\begin{bmatrix}\boldsymbol{v}\\ \boldsymbol{z}\\ \boldsymbol{\eta}\end{bmatrix}. \quad (26)$$

The transformed system has the following dynamics

$$\begin{bmatrix}\dot{\boldsymbol{x}}_v\\ \dot{\boldsymbol{x}}_z\\ \dot{\boldsymbol{x}}_\eta\end{bmatrix} = \begin{bmatrix}\boldsymbol{0} & \boldsymbol{0} & \boldsymbol{0}\\ \boldsymbol{L}'_3 & \boldsymbol{0} & \boldsymbol{0}\\ \boldsymbol{0} & \boldsymbol{I}_{3n} & \boldsymbol{0}\end{bmatrix}\begin{bmatrix}\boldsymbol{x}_v\\ \boldsymbol{x}_z\\ \boldsymbol{x}_\eta\end{bmatrix} + \begin{bmatrix}\hat{\boldsymbol{R}}\\ \boldsymbol{0}\\ \boldsymbol{0}\end{bmatrix}\boldsymbol{u} + \begin{bmatrix}\boldsymbol{I}_{3n}\\ \boldsymbol{0}\\ \boldsymbol{0}\end{bmatrix}\boldsymbol{d} + \begin{bmatrix}\boldsymbol{0}\\ \boldsymbol{I}_{3n}\\ \boldsymbol{0}\end{bmatrix}\dot{\boldsymbol{z}}_{ref}. \quad (27)$$

Following the works of [6], it can be proven that using LQR tools for an individual drone, a control law $\boldsymbol{u} = -\hat{\boldsymbol{R}}^T\hat{\boldsymbol{K}}_v\boldsymbol{x}_v = -\hat{\boldsymbol{R}}^T\hat{\boldsymbol{K}}_v\hat{\boldsymbol{R}}\boldsymbol{v}$ makes the velocity of each vehicle stable around $\boldsymbol{0}$. With this in consideration, the following can be stated.

Lemma 6 *Consider the control law applied to the system (25)*

$$\boldsymbol{u} = -\begin{bmatrix}\hat{\boldsymbol{R}}^T\hat{\boldsymbol{K}}_v\hat{\boldsymbol{R}} & \hat{\boldsymbol{R}}^T\hat{\boldsymbol{K}}_z & \hat{\boldsymbol{R}}^T\hat{\boldsymbol{K}}_\eta\end{bmatrix}\begin{bmatrix}\boldsymbol{v}\\ \boldsymbol{z}\\ \boldsymbol{\eta}\end{bmatrix}, \quad (28)$$

1. *The control law can be stable for appropriate gains $\hat{\boldsymbol{K}}_v$, $\hat{\boldsymbol{K}}_z$ and $\hat{\boldsymbol{K}}_\eta$;*
2. *The control law is able to reject constant disturbances $\boldsymbol{d}$ in the velocity and the position of every vehicle;*
3. *The control law allows the tracking of a ramp signal in $\boldsymbol{z}_{ref}$ with no stationary error in every vehicle.*

Proof The individual controller of each vehicle has a transformed dynamic equation represented by

$$\dot{\boldsymbol{x}}_v = -\boldsymbol{K}_{v_i}\boldsymbol{x}_v. \tag{29}$$

Assume that each vehicle has a similar stable controller but with different gains. Let λ_{v_+} denote the majorant of the real part of the eigenvalues of all of these controllers. The outer loop

$$\begin{bmatrix}\dot{\boldsymbol{x}}_v\\ \dot{\boldsymbol{x}}_z\end{bmatrix} = \begin{bmatrix}\boldsymbol{0} & -\hat{\boldsymbol{K}}_z\\ \boldsymbol{L}_3' & \boldsymbol{0}\end{bmatrix}\begin{bmatrix}\boldsymbol{x}_v\\ \boldsymbol{x}_z\end{bmatrix} \tag{30}$$

has eigenvalues $\sqrt{\mu}e^{\frac{\pi+2k\pi}{2}i}$ where μ are the eigenvalues of $\hat{\boldsymbol{K}}_i\boldsymbol{L}_3'$, with $k\in\mathbb{Z}$. Assuming that μ are real valued, then the majorant of the real part of the eigenvalues of the system above is $\lambda_{z_+}=0$. Similarly, the outer loop

$$\begin{bmatrix}\dot{\boldsymbol{x}}_v\\ \dot{\boldsymbol{x}}_z\\ \dot{\boldsymbol{x}}_\eta\end{bmatrix} = \begin{bmatrix}\boldsymbol{0} & \boldsymbol{0} & -\hat{\boldsymbol{K}}_\eta\\ \boldsymbol{L}_3' & \boldsymbol{0} & \boldsymbol{0}\\ \boldsymbol{0} & \boldsymbol{I}_{3n} & \boldsymbol{0}\end{bmatrix}\begin{bmatrix}\boldsymbol{x}_v\\ \boldsymbol{x}_z\\ \boldsymbol{x}_\eta\end{bmatrix} \tag{31}$$

has eigenvalues $\sqrt[3]{\nu}e^{\frac{\pi+2k\pi}{3}i}$ where ν are the eigenvalues of $\hat{\boldsymbol{K}}_\eta\boldsymbol{L}_3'$, with $k\in\mathbb{Z}$. With the assumption that ν are real, the majorant of the real part of the eigenvalues of the previous system is $\lambda_{\eta_+}=\frac{\sqrt[3]{\mathrm{maj}\{\nu\}}}{2}$. From corollary 1, the application of the proposed control law to system (27) makes the global system to have eigenvalues with the real part majored by $\lambda_{v_+}+\lambda_{z_+}+\lambda_{\eta_+}$. Therefore, it is possible to choose the gains $\hat{\boldsymbol{K}}_v$, $\hat{\boldsymbol{K}}_z$ and $\hat{\boldsymbol{K}}_\eta$ such that the system is stable.

Furthermore, apply the control law in (27) and perform the Laplace transform. The system in the frequency domain can be written as

$$\begin{bmatrix}\boldsymbol{x}_v(s)\\ \boldsymbol{x}_z(s)\\ \boldsymbol{x}_\eta(s)\end{bmatrix} = \boldsymbol{M}(s)^{-1}\begin{bmatrix}\boldsymbol{I}_{3n} & \boldsymbol{0}\\ \boldsymbol{0} & s\boldsymbol{I}_{3n}\\ \boldsymbol{0} & \boldsymbol{0}\end{bmatrix}\begin{bmatrix}\boldsymbol{d}(s)\\ \boldsymbol{z}_{ref}(s)\end{bmatrix}, \tag{32}$$

with

$$\boldsymbol{M}(s) = \begin{bmatrix}s\boldsymbol{I}_{3n}+\hat{\boldsymbol{K}}_v & \hat{\boldsymbol{K}}_z & \hat{\boldsymbol{K}}_\eta\\ -\boldsymbol{L}_3' & s\boldsymbol{I}_{3n} & \boldsymbol{0}\\ \boldsymbol{0} & -\boldsymbol{I}_{3n} & s\boldsymbol{I}_{3n}\end{bmatrix}. \tag{33}$$

The final value theorem states that, if the system is stable,

$$\lim_{t\to\infty}\begin{bmatrix}\boldsymbol{x}_v(t)\\ \boldsymbol{x}_z(t)\\ \boldsymbol{x}_\eta(t)\end{bmatrix} = \lim_{s\to 0} s\begin{bmatrix}\boldsymbol{x}_v(s)\\ \boldsymbol{x}_z(s)\\ \boldsymbol{x}_\eta(s)\end{bmatrix}. \tag{34}$$

Considering a constant disturbance $\boldsymbol{d}(s)=\frac{\boldsymbol{c_d}}{s}$ and a ramp reference $\boldsymbol{z}_{ref}(s)=\frac{\boldsymbol{c}_z}{s^2}$ and substituting in (32), the above limit becomes

$$\lim_{s\to 0} s\begin{bmatrix}\boldsymbol{x}_v(s)\\ \boldsymbol{x}_z(s)\\ \boldsymbol{x}_\eta(s)\end{bmatrix} = \boldsymbol{M}(0)^{-1}\begin{bmatrix}\boldsymbol{I}_{3n} & \boldsymbol{0}\\ \boldsymbol{0} & \boldsymbol{I}_{3n}\\ \boldsymbol{0} & \boldsymbol{0}\end{bmatrix}\begin{bmatrix}\boldsymbol{c}_d\\ \boldsymbol{c}_z\end{bmatrix}. \tag{35}$$

Using Schur's formula, one can compute

$$\boldsymbol{M}(0)^{-1} = \begin{bmatrix}\boldsymbol{0} & -\boldsymbol{L}_3'^{-1} & \boldsymbol{0}\\ \boldsymbol{0} & \boldsymbol{0} & -\boldsymbol{I}_{3n}\\ \hat{\boldsymbol{K}}_\eta^{-1} & \hat{\boldsymbol{K}}_\eta^{-1}\hat{\boldsymbol{K}}_v\boldsymbol{L}_3'^{-1} & \hat{\boldsymbol{K}}_\eta^{-1}\hat{\boldsymbol{K}}_z\end{bmatrix}. \tag{36}$$

In conclusion,

$$\lim_{t\to\infty}\begin{bmatrix}\boldsymbol{x}_v(t)\\ \boldsymbol{x}_z(t)\\ \boldsymbol{x}_\eta(t)\end{bmatrix} = \begin{bmatrix}\boldsymbol{0} & -\boldsymbol{L}_3'^{-1}\\ \boldsymbol{0} & \boldsymbol{0}\\ \hat{\boldsymbol{K}}_\eta^{-1} & \hat{\boldsymbol{K}}_\eta^{-1}\hat{\boldsymbol{K}}_v\boldsymbol{L}_3'^{-1}\end{bmatrix}\begin{bmatrix}\boldsymbol{c}_d\\ \boldsymbol{c}_z\end{bmatrix}. \tag{37}$$

Attending to the fact that $\boldsymbol{z}(t)=\boldsymbol{x}_z(t)$ and that $\boldsymbol{v}(t)=\hat{\boldsymbol{R}}^T\boldsymbol{x}_v(t)$, statements 2. and 3. are proven. □

Remark 4 Assume that the matrices $\hat{\boldsymbol{K}}_v$, $\hat{\boldsymbol{K}}_z$ and $\hat{\boldsymbol{K}}_\eta$ are diagonal with the same value, k_v, k_z and k_η, respectively. The global feedback law will make the eigenvalues of (27) be majored by $-k_v+\frac{\sqrt[3]{k_\eta\lambda_{L_+}}}{2}$, where λ_{L_+} is the largest eigenvalue of $\boldsymbol{L}'$. Thus, a condition for stability, in this case, is to have

$$k_v > \frac{\sqrt[3]{k_\eta\lambda_{L_+}}}{2}. \tag{38}$$

This lemma shows that the proposed control law makes the formation robust, giving not only the capability of the vehicles rejecting their own constant disturbances and tracking errors, but also rejecting the influence of those factors when applied to neighbouring vehicles. With this control law, it is possible to extract what should be the command given to the quadrotor's actuators, as derived in [6]. Let $\boldsymbol{u}_i^*$ denote the input of the i-th vehicle calculated through the control law in theorem 6.

Lemma 7 *If $\boldsymbol{u}_i^*$ satisfies the condition*

$$\|\boldsymbol{u}_i^*\| \le g, \tag{39}$$

then it is always possible to extract the thrust magnitude from

$$T_i = m\left|\sqrt{g^2-\boldsymbol{u}_{i_1}^{*2}-\boldsymbol{u}_{i_2}^{*2}}-\boldsymbol{u}_{i_3}^*\right|. \tag{40}$$

Furthermore define $\boldsymbol{b}_3=\frac{\boldsymbol{u}_i^*+\frac{T_i}{m}\boldsymbol{e}_3}{\|\boldsymbol{u}_i^*+\frac{T_i}{m}\boldsymbol{e}_3\|}$ and $\boldsymbol{b}_d=\boldsymbol{e}_3$. With $\boldsymbol{b}_2=\frac{\boldsymbol{b}_3\times\boldsymbol{b}_d}{\|\boldsymbol{b}_3\times\boldsymbol{b}_d\|}$ and $\boldsymbol{b}_1=\frac{\boldsymbol{b}_2\times\boldsymbol{b}_3}{\|\boldsymbol{b}_2\times\boldsymbol{b}_3\|}$, let $\boldsymbol{R}_1=\begin{bmatrix}\boldsymbol{b}_1 & \boldsymbol{b}_2 & \boldsymbol{b}_3\end{bmatrix}$. Similarly, let $\boldsymbol{c}_3=\boldsymbol{e}_3$ and $\boldsymbol{c}_d=\begin{bmatrix}\cos\psi_d & \sin\psi_d & 0\end{bmatrix}^T$, where ψ_d is the desired yaw angle. With $\boldsymbol{c}_2=\frac{\boldsymbol{c}_3\times\boldsymbol{c}_d}{\|\boldsymbol{c}_3\times\boldsymbol{b}_d\|}$ and $\boldsymbol{c}_1=\frac{\boldsymbol{c}_2\times\boldsymbol{c}_3}{\|\boldsymbol{c}_2\times\boldsymbol{c}_3\|}$, define $\boldsymbol{R}_2=\begin{bmatrix}\boldsymbol{c}_1 & \boldsymbol{c}_2 & \boldsymbol{c}_3\end{bmatrix}$. Finally, the desired attitude may be extracted from the control law.

Lemma 8 *The desired attitude for the vehicle is given by*

$$\boldsymbol{R}_{d_i} = \boldsymbol{R}_2\boldsymbol{R}_1^T. \tag{41}$$

Let $\boldsymbol{W} = \begin{bmatrix} 0 & -1 & 0 \\ 1 & 0 & 0 \end{bmatrix}$. *With*

$$\boldsymbol{\omega}_1 = \begin{bmatrix} \boldsymbol{W}\boldsymbol{R}_1^T \dot{\boldsymbol{b}}_3 \\ -\boldsymbol{b}_1^T \dot{\boldsymbol{b}}_2 \end{bmatrix} \tag{42}$$

and

$$\boldsymbol{\omega}_2 = \begin{bmatrix} 0 \\ 0 \\ -\boldsymbol{c}_1^T \dot{\boldsymbol{c}}_2 \end{bmatrix}, \tag{43}$$

the desired angular velocity is simply

$$\boldsymbol{\omega}_{d_i} = \boldsymbol{R}_1(\boldsymbol{\omega}_2 - \boldsymbol{\omega}_1). \tag{44}$$

The controller for the position must give a reference to the attitude due to the dynamics of the vehicle, leading to the conclusion that an attitude controller is crucial to achieve position tracking, which will be addressed later on. To summarize this subsection, a block diagram for the position controller of a single vehicle is shown in Fig. 2

4.2 Attitude Tracking Control

Suppose the desired attitude for the i-th vehicle is $\boldsymbol{q}_{d_i} = \begin{bmatrix} \boldsymbol{q}_{vd_i}^T & q_{4d_i} \end{bmatrix}^T$. Following [6], the quaternion error may be defined as

$$\boldsymbol{e}_{q_i} = \boldsymbol{\Xi}(\boldsymbol{q}_{d_i})\boldsymbol{q}_i, \tag{45}$$

with $\boldsymbol{\Xi}(\boldsymbol{q}) = \begin{bmatrix} q_4\boldsymbol{I}_3 + [\boldsymbol{q}_v\times] \\ -\boldsymbol{q}_v^T \end{bmatrix}$. In the body frame, the angular velocity error can be defined as

$$\boldsymbol{e}_{\omega_i} = \boldsymbol{\omega}_i - \boldsymbol{\Sigma}(\boldsymbol{e}_{q_i})^{-1}\boldsymbol{\Sigma}(\boldsymbol{e}_{q_i})^T\boldsymbol{\omega}_{d_i}, \tag{46}$$

with $\boldsymbol{\Sigma}(\boldsymbol{e}_{q_i}) = \begin{bmatrix} \boldsymbol{q}_{d_i}^T\boldsymbol{q}_i & -\boldsymbol{e}_{q_{3i}} & \boldsymbol{e}_{q_{2i}} \\ \boldsymbol{e}_{q_{3i}} & \boldsymbol{q}_{d_i}^T\boldsymbol{q}_i & -\boldsymbol{e}_{q_{1i}} \\ -\boldsymbol{e}_{q_{2i}} & \boldsymbol{e}_{q_{1i}} & \boldsymbol{q}_{d_i}^T\boldsymbol{q}_i \end{bmatrix}$. Lastly, consider an integrative state $\dot{\boldsymbol{\xi}}_i = \boldsymbol{e}_{q_i}$. From equations (3) and (4) and deriving equations (45) and (46), the following system is obtained ([6]),

$$\begin{cases} \dot{\boldsymbol{e}}_{q_i} = \frac{1}{2}\boldsymbol{\Sigma}(\boldsymbol{e}_{q_i})\boldsymbol{e}_{\omega_i} \\ \dot{\boldsymbol{e}}_{\omega_i} = -\boldsymbol{J}^{-1}[\boldsymbol{\omega}_i\times]\boldsymbol{J}\boldsymbol{\omega}_i + \boldsymbol{J}^{-1}\boldsymbol{\tau}_i \\ \qquad\quad - \dfrac{d}{dt}(\boldsymbol{\Sigma}(\boldsymbol{e}_{q_i})^{-1}\boldsymbol{\Sigma}(\boldsymbol{e}_{q_i})^T\boldsymbol{\omega}_{d_i}) \\ \dot{\boldsymbol{\xi}}_i = \boldsymbol{e}_{q_i} \end{cases}. \tag{47}$$

By defining

$$\begin{aligned} \boldsymbol{\tau}_{n_i} =& -\boldsymbol{J}^{-1}[\boldsymbol{\omega}_i\times]\boldsymbol{J}\boldsymbol{\omega}_i + \boldsymbol{J}^{-1}\boldsymbol{\tau}_i \\ & - \frac{d}{dt}(\boldsymbol{\Sigma}(\boldsymbol{e}_{q_i})^{-1}\boldsymbol{\Sigma}(\boldsymbol{e}_{q_i})^T\boldsymbol{\omega}_{d_i}), \end{aligned} \tag{48}$$

the equations may be written in space-state form,

$$\begin{bmatrix} \dot{\boldsymbol{e}}_{q_i} \\ \dot{\boldsymbol{e}}_{\omega_i} \\ \dot{\boldsymbol{\xi}}_i \end{bmatrix} = \begin{bmatrix} \boldsymbol{0} & \frac{1}{2}\boldsymbol{\Sigma}(\boldsymbol{e}_{q_i}) & \boldsymbol{0} \\ \boldsymbol{0} & \boldsymbol{0} & \boldsymbol{0} \\ \boldsymbol{I}_3 & \boldsymbol{0} & \boldsymbol{0} \end{bmatrix} \begin{bmatrix} \boldsymbol{e}_{q_i} \\ \boldsymbol{e}_{\omega_i} \\ \boldsymbol{\xi}_i \end{bmatrix} + \begin{bmatrix} \boldsymbol{0} \\ \boldsymbol{I}_3 \\ \boldsymbol{0} \end{bmatrix} \boldsymbol{\tau}_{n_i}. \tag{49}$$

With the application of the Lyapunov Transform proposed in [6]

$$\begin{bmatrix} \boldsymbol{x}_{q_i} \\ \boldsymbol{x}_{\omega_i} \\ \boldsymbol{x}_{\xi_i} \end{bmatrix} = \begin{bmatrix} \boldsymbol{I}_3 & \boldsymbol{0} & \boldsymbol{0} \\ \boldsymbol{0} & \boldsymbol{\Sigma}(\boldsymbol{e}_{q_i}) & \boldsymbol{0} \\ \boldsymbol{0} & \boldsymbol{0} & \boldsymbol{I}_3 \end{bmatrix} \begin{bmatrix} \boldsymbol{e}_{q_i} \\ \boldsymbol{e}_{\omega_i} \\ \boldsymbol{\xi}_i \end{bmatrix}, \tag{50}$$

the transformed space-state system is

$$\begin{bmatrix} \dot{\boldsymbol{x}}_{q_i} \\ \dot{\boldsymbol{x}}_{\omega_i} \\ \dot{\boldsymbol{x}}_{\xi_i} \end{bmatrix} = \begin{bmatrix} \boldsymbol{0} & \frac{1}{2}\boldsymbol{I}_3 & \boldsymbol{0} \\ \boldsymbol{0} & \boldsymbol{0} & \boldsymbol{0} \\ \boldsymbol{I}_3 & \boldsymbol{0} & \boldsymbol{0} \end{bmatrix} \begin{bmatrix} \boldsymbol{x}_{q_i} \\ \boldsymbol{x}_{\omega_i} \\ \boldsymbol{x}_{\xi_i} \end{bmatrix} + \begin{bmatrix} \boldsymbol{0} \\ \boldsymbol{I}_3 \\ \boldsymbol{0} \end{bmatrix} \boldsymbol{\tau}_{l_i}, \tag{51}$$

where

$$\boldsymbol{\tau}_{l_i} = \boldsymbol{\Sigma}(\boldsymbol{e}_{q_i})\boldsymbol{\tau}_{n_i} + \boldsymbol{\Xi}(\boldsymbol{q}_{d_i})^T\boldsymbol{\Xi}(\dot{\boldsymbol{q}}_i)\boldsymbol{\Sigma}(\boldsymbol{e}_q)^{-1}\boldsymbol{x}_{\omega_i}. \tag{52}$$

As proven in [6], it is possible to design a controller for (51) through LQR that renders (49) almost globally exponentially stable. If the obtained optimal control law is $\boldsymbol{\tau}_l^* = -\boldsymbol{K}_q\boldsymbol{x}_{q_i} - \boldsymbol{K}_\omega\boldsymbol{x}_{\omega_i} - \boldsymbol{K}_\xi\boldsymbol{x}_{\xi_i}$, then, applying the reverse transformations,

$$\begin{aligned} \boldsymbol{\tau}_i^* =& [\boldsymbol{\omega}_i\times]\boldsymbol{J}\boldsymbol{\omega}_i + \boldsymbol{J}\frac{d}{dt}(\boldsymbol{\Sigma}(\boldsymbol{e}_{q_i})^{-1}\boldsymbol{\Sigma}(\boldsymbol{e}_{q_i})^T\boldsymbol{\omega}_{d_i}) + \\ & \boldsymbol{J}\boldsymbol{\Sigma}(\boldsymbol{e}_{q_i})^{-1}\left(\boldsymbol{\tau}_{l_i}^* - \boldsymbol{\Xi}(\boldsymbol{q}_{d_i})^T\boldsymbol{\Xi}(\dot{\boldsymbol{q}}_i)\boldsymbol{e}_{\omega_i}\right). \end{aligned} \tag{53}$$

With this final equation, the whole controller is now fully developed. To summarize this section, a block diagram for the attitude controller of an individual vehicle is presented in Fig. 3.

5 Simulation Results

For the simulation, each quadrotor was chosen to have a mass of $m = 0.5$ Kg and an inertia matrix of $\boldsymbol{J} = \text{diag}(0.0027, 0.0029, 0.0053)$ Kg.m^2. Five vehicles will be considered and it is assumed that the information flows between the vehicles as

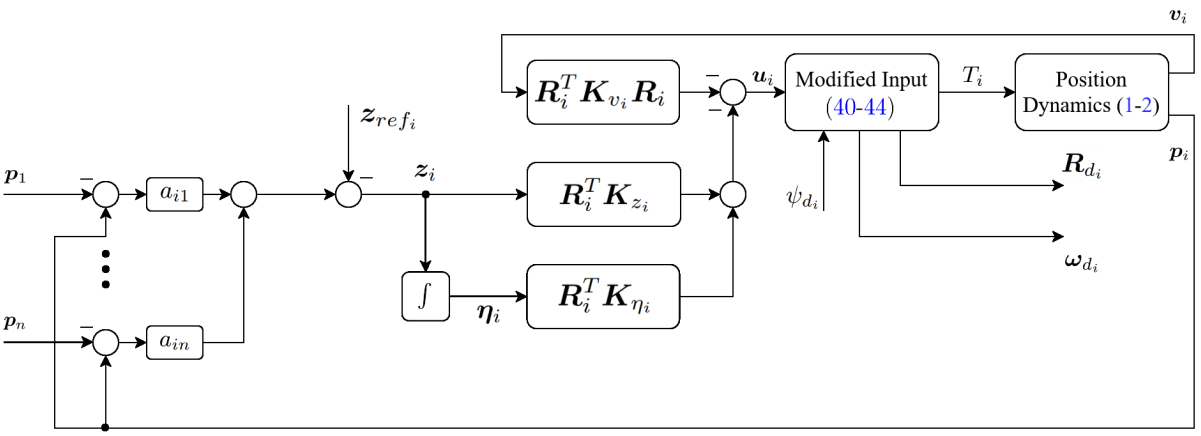

Fig. 2: Block Diagram of the Position Controller

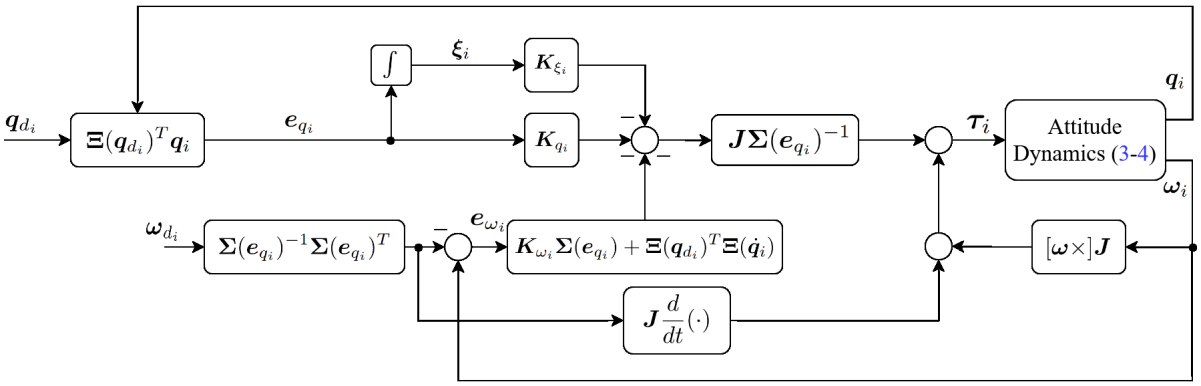

Fig. 3: Block Diagram of the Attitude Controller

shown in Fig. 4. The vehicles must maintain a V-formation always aligned with the yaw of the first quadrotor, as shown in the same figure. Furthermore, only vehicle 1 will receive information about the reference trajectory. The five drones start

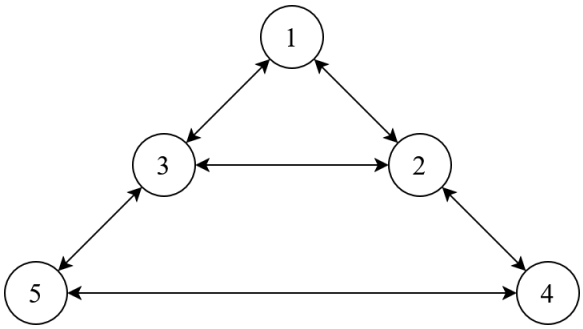

Fig. 4: Formation Diagram

at, respectively, positions $\boldsymbol{p}_{01} = \begin{bmatrix}-2 & 3 & 0\end{bmatrix}^T$ m, $\boldsymbol{p}_{02} = \begin{bmatrix}2 & -4 & 0\end{bmatrix}^T$ m, $\boldsymbol{p}_{03} = \begin{bmatrix}2 & 2 & 0\end{bmatrix}^T$ m, $\boldsymbol{p}_{04} = \begin{bmatrix}0 & 0 & 0\end{bmatrix}^T$ m and $\boldsymbol{p}_{05} = \begin{bmatrix}1 & 1 & 0\end{bmatrix}^T$ m. At $t = 2$ s, the vehicles start to climb to a height of 2 m while going into formation and, starting at $t = 10$ s, the reference trajectory that each vehicle should follow is represented, in the X-Y plane, in Fig. 5, beginning in the origin, at a constant height of 2 m and a constant velocity of 0.5 m/s.

Constant perturbations will be given to the vehicles starting at certain time instants and lasting until the end of the simulation. Starting at $t = 40$ s, drone 1 will have a constant perturbation of $d_1 = \begin{bmatrix}2 & 0 & -2\end{bmatrix}^T$. At $t = 80$ s, drone 2 will receive a constant perturbation of $d_2 = \begin{bmatrix}0 & -2.5 & 0\end{bmatrix}^T$ and drone 3 a perturbation of $d_3 = \begin{bmatrix}0 & 2.5 & 0\end{bmatrix}^T$. Finally,

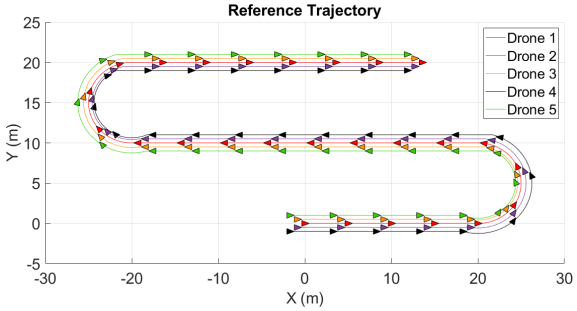

Fig. 5: Reference trajectory in the X-Y plane

at $t = 100$ s, drone 4 will receive a perturbation of $d_4 = \begin{bmatrix}2 & -1.5 & 1.5\end{bmatrix}^T$ and drone 5 one of $d_5 = \begin{bmatrix}-2 & 1.5 & 1.5\end{bmatrix}^T$. The reference for the yaw will be such that the front of the vehicles are aligned with the reference velocity vectors.

As for the controller, each vehicle will have the following position gains as per the notation used in previous sections: $\boldsymbol{K}_{v_i} = \text{diag}(5,5,5)$; $\boldsymbol{K}_{z_i} = \text{diag}(8,8,8)$; $\boldsymbol{K}_{\eta_i} = \text{diag}(5,5,5)$. For the individual attitude controller, the gains are calculated with a LQR for system (51), with the weighting matrices $\boldsymbol{Q} = \text{diag}(\boldsymbol{q}_q, \boldsymbol{q}_\omega, \boldsymbol{q}_\xi)$ and $\boldsymbol{R} = \text{diag}(92,92,92)$, where $\boldsymbol{q}_q = (65,65,65) \times 10^4$, $\boldsymbol{q}_\omega = (5,5,5) \times 10^4$ and $\boldsymbol{q}_\xi = (30,30,30) \times 10^7$.

Lastly, in order to evaluate the controller performance facing sensor imperfections, white noise was added to the position sensors of every drone with a standard deviation of 15 cm in every coordinate. These sensors also suffer from a delay of 10 ms. The velocity sensors will also suffer from white noise with a standard deviation of 15 cm/s.

From Figs. 6a, 6b and 6c, it is possible to draw three conclusions in line with what is stated in theorem 6. One can see that the control law is, in fact, stable. It can also be seen that the effect of constant disturbances on a certain vehicle is quickly rejected by every vehicle from the formation. Lastly, in straight segments of the trajectory, it can be seen that the tracking error converges to zero in all vehicles, albeit slowly in this case, which confirms the null static error on constant velocity trajectories. The presence of noise and time delays, despite their high values and the absence of a state estimator, is very well attenuated as it can be observed in the plots. A video of the simulated position tracking in real time is available at https://www.youtube.com/watch?v=JRY49y6mw5U.

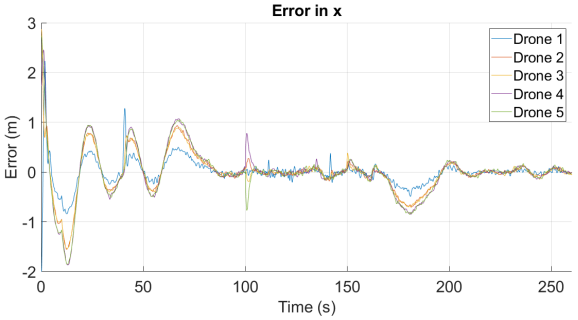

(a) Error in x

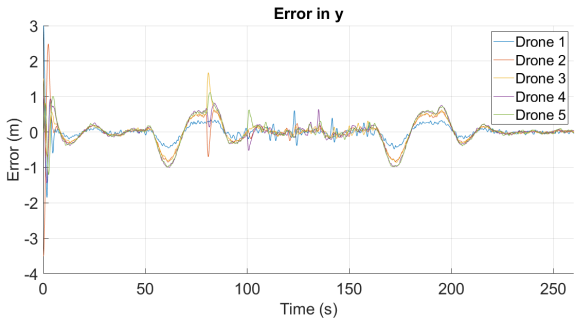

(b) Error in y

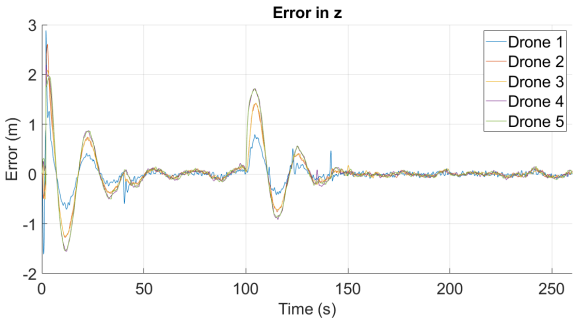

(c) Error in z

Fig. 6: Position tracking errors

The plots in Figs. 7a, 7b and 7c also allow the conclusion that the attitude is stable and that the vehicles track very well the reference yaw. However, the sensor imperfections do have a significant effect on the attitude of the quadrotors, namely on the yaw of the vehicles when it is around π rad. The pitch and roll of the vehicles remain roughly bounded between -0.2 rad and 0.2 rad, which is satisfactory. The study of the effect of sensor imperfections on the proposed control solution and the development of an adequate observer should be topics for future works.

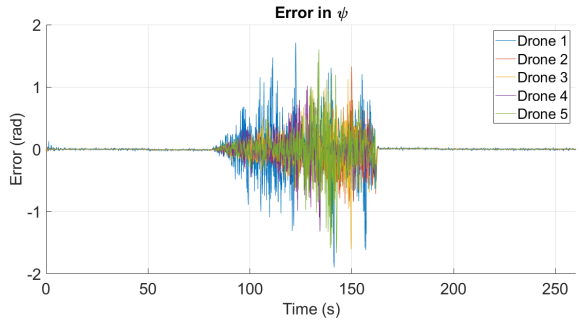

(a) Error in the yaw angle

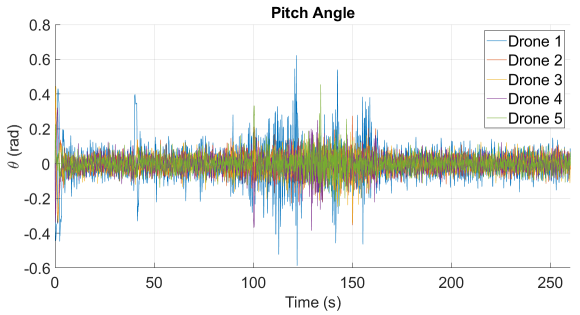

(b) Pitch angle

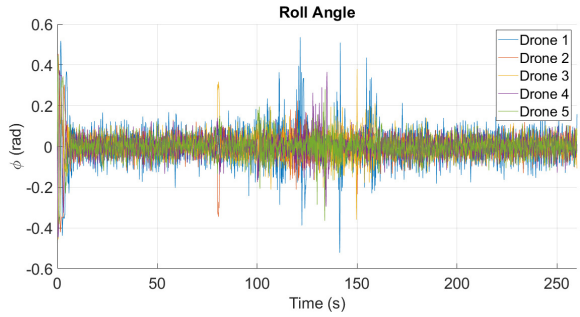

(c) Roll angle

Fig. 7: Attitude of the vehicles

As a final remark, by doing these simulations, one might find that the performance of the formation is as better as denser is the communication graph between the vehicles, as is to be expected. With the same logic, if the reference trajectory is known to more vehicles, then the performance further enhances. For instance, with this configuration, a compromise must be made for drone 1 whether it should prioritize following the trajectory or to not stray much away from its peers, which naturally degrades the overall performance. The parameters that assert this compromise are the weights of the virtual drone when constructing matrix $\boldsymbol{L}'$. These may be topics to be addressed in a future work.

6 Conclusion

This article presented a distributed trajectory tracking controller for a group of quadrotor vehicles, with optimal steady-state properties and due robustness facing disturbances. The dynamics are written in the body frame of each vehicle in order to allow the direct usage of sensor measurements and, resorting to Lyapunov transforms, it was possible to render the global position and attitude system LTI and make use of linear control tools such as LQR while maintaining the robust properties of non-linear controllers. Furthermore, it was also presented sufficient conditions for stability of groups of vehicles generalized to all types of information flow graphs and all types of vehicles, as long as they have stable internal dynamics. With a robust internal controller and a solid theory for the cooperation of multiple vehicles, an outer loop for the controller was designed which is proven to be stable and allow for trajectory tracking, given that the information graphs are strongly connected and undirected. The controller is also shown to be able to follow trajectories at constant velocities with null steady-state and to reject constant unknown perturbations in every vehicle. Lastly, simulation results were presented to experimentally confirm the results theoretically derived.

(**??**-**??**)

References

[1] Fax, J.A., Murray, R.M.: Information flow and cooperative control of vehicle formations. IEEE Transactions on Automatic Control **49**(9), 1456–1476 (2004) https://doi.org/10.1109/TAC.2004.834433

[2] Olfati-Saber, R., Murray, R.M.: Consensus problems in networks of agents with switching topology and time-delays. IEEE Transactions on Automatic Control **49**, 1520–1533 (2004) https://doi.org/10.1109/TAC.2004.834113

[3] Olfati-Saber, R., Fax, J.A. and Murray, R.M.: Consensus and cooperation in networked multi-agent systems. Proceedings of

the IEEE **95**(1), 215–233 (2007) https://doi.org/10.1109/JPROC.2006.887293

[4] Cortes, J., Martinez, S. and Bullo, F: Robust rendezvous for mobile autonomous agents via proximity graphs in arbitrary dimensions. IEEE Transactions on Automatic Control **51**(8), 1289–1298 (2006) https://doi.org/10.1109/TAC.2006.878713

[5] Dunbar, W.B., Murray, R.M.: Distributed receding horizon control for multi-vehicle formation stabilization. Automatica **42**(4), 549–558 (2006) https://doi.org/10.1016/j.automatica.2005.12.008

[6] Madeiras, J., Cardeira, C. and Oliveira, P.: Position and attitude tracking controllers using lyapunov transformations for quadrotors. Journal of Intelligent & Robotic Systems **110**(9) (2024) https://doi.org/10.1007/s10846-023-02016-9

[7] Brockett, R.W.: Finite Dimensional Linear Systems. John Wiley and Sons, Inc., New York (1970). https://doi.org/10.1137/1.9781611973884

[8] Gamagedara, K., Lee, T. and Snyder, M.: Quadrotor state estimation with imu and delayed real-time kinematic gps. IEEE Transactions on Aerospace and Electronic Systems **57**(5), 2661–2673 (2021) https://doi.org/10.1109/TAES.2021.3061795

[9] Marcus, M., Minc, H.: A Survey of Matrix Theory and Matrix Inequalities. Allyn and Bacon, Michigan (1962)